IMPEDANCE FIELD IN SUBMICRON n^+nn^+ InP DIODES

V.Mitin[1)], V. Gružinskis[2)], E. Starikov[2)], P. Shiktorov[2)], L. Reggiani[3)], L. Varani [4)]

[1)] *Department of ECE Wayne State University Detroit, MI 48202, USA*

[2)] *Semiconductor Physics Institute A. Goštauto 11, 2600 Vilnius, Lithuania*

[3)] *Dipartimento di Fisica Università di Modena, Via Campi 213/A, 41100 Modena, Italy*

[4)] *Centre d'Electronique de Montpellier, Université des Sciences et Techniques du Languedoc, 34095 Montpellier Cedex 5, France*

Abstract

The physical processes responsible for microwave power generation in submicron n^+nn^+ InP diodes are analyzed through the spatial profiles of the impedance-field spectrum calculated by a closed hydrodynamic approach. The usual subdivision of the n-region into a dead and active zone is carried out. The dead zone is found to manifest itself as a purely real resistance which is practically independent of the frequency. One or more spatial zones which are responsible for the generation are shown to be formed in the active region of the diode. By reducing the n-region length the additivity of the contributions from each part of the device into the generation spectrum is proven.

I. INTRODUCTION

Near-micron n^+nn^+ InP diodes are widely used in modern electronics as generators in the millimeter region of the electromagnetic spectrum [1,2]. To improve the high-frequency performance of these generators various doping profiles [2,3] and a reduction of the n-region length [4,5] are usually suggested. For a proper choice of these parameters and to clarify some problems related to their design, an appropriate physical modeling of these devices is mandatory. To provide the detailed description of the physical processes responsible for the diode performance a quantitative analysis of the parameters which allow for a spatial analysis of various physical quantities has to be preferred. Indeed, by allowing one to construct a spatial map of the device properties of interest, the designing of the device is significantly facilitated. The main aim of this paper is to demonstrate that the impedance field can be successfully used for this sake.

II. THE IMPEDANCE FIELD APPROACH

When considering n^+nn^+ diodes as microwave power generators, the characteristics which describe the capabilities of the device to amplify small perturbations are of great importance. Under current-driven operation, these capabilities can be rigorously described through the local impedance-field, which is given by the ratio of the Fourier components of the local electric-field $\delta E_\omega(x)$ and the total current $\delta j_\omega(x)$ at circular frequency $\omega = 2\pi f$ in point x as: $\nabla Z(\omega, x) = \delta E_\omega(x)/\delta j_\omega(x)$. Since for the one-dimensional structure considered here, the total current is constant in space, the impedance field reflects spatial behavior of possible perturbations of the local electric field caused by harmonic perturbation of j. Integration of the impedance field throughout the structure gives the small-signal impedance of the whole diode, $Z(\omega) = \int_0^l \nabla Z(\omega, x)dx$. Since the impedance field describes the additive contributions which every point of the diode gives to the small-signal impedance, $\nabla Z(\omega, x)$ can be used for a detailed spatial analysis of the diode performance. To simulate the carrier transport in submicron n^+nn^+ InP diodes the full hydrodynamic model [4-10] based on the carrier concentration, drift velocity and mean energy conservation equations coupled with the Poisson equation for the self-consistent electric field is used. This model was demonstrated to provide an excellent agreement with the Monte Carlo calculations for both bulk semiconductors [7-9] and short n^+nn^+ structures [4-6,10]. In the present paper we apply it to study the contributions of the various parts of the diode to $Z(\omega)$ and its dependence on reducing the diode length. For this sake we use an impulsive procedure [10] which enables us to obtain under the current-driven operation simultaneously the spectra of both $\nabla Z(\omega, x)$ and $Z(\omega)$ in the frequency range of interest.

III. RESULTS AND DISCUSSION

We consider a n^+nn^+ structure at $T = 300\ K$ with parameters which are typical of to-date diode generators [1,2]: the n-region length $l_n = 1\ \mu m$, $n = 2\times10^{16}\ cm^{-3}$, $n^+ = 10^{18}\ cm^{-3}$. Abrupt homojunctions between n and n^+ regions are assumed. The cathode and anode n^+-region lengths are taken to be 0.1 and $0.3\mu m$, respectively.

Under the current driven operation the electron heating in the diode can be considered (to somewhat extent) as a local property. This is illustrated in Fig. 1, which presents a stationary profiles of the drift velocity in the structures with different lengths of the n region calculated for the same total current j_0. Reduction of the n region length does not change the velocity profile in the common region and it looks as a cut of the corresponding part of n-region which is on the anode side. For the case of $l_n = 1\ \mu m$ ($U_d = 8\ V$) the velocity overshoot results in the spatial negative differential-conductivity (SNDC) in the space region $0.3 < x < 1.1\ \mu m$, where the drift velocity decreases with increasing the spatial coordinate. The real part of the small-signal impedance calculated for the considered n^+nn^+ structure is reported for different lengths of the n-region in Fig. 2. For the case of $l_n = 1\ \mu m$ (see curve 1), the amplification condition, $Re[Z(f)] < 0$, is fulfilled inside the two bands: $f = 70 \div 200$ and $250 \div 340\ GHz$ where microwave power generation is possible. We remark that, by shortening the n-region, the condition for amplification shifts to high frequencies, as expected. Figures 3 (a) and (b) report the spatial profile respectively of the real and imaginary parts of the impedance field for the structure with $l_n = 1\ \mu m$. Curves 1,2, and 3 correspond, respectively, to the frequencies $f_1 = 55\ GHz$, $f_2 = 125\ GHz$, and $f_3 = 290\ GHz$. As it follows from Fig. 3, $\nabla Z(f, x)$ is practically independent from frequency in the near-cathode area of the n-region ($x = 0.10 \div 0.30\ \mu m$).

From the comparison with curve 1 of Fig. 1, we find that this is the region where the drift velocity exhibits a sharp increase up to its maximum value. This space region is usually called as the dead zone of short diodes. Comparing Figs. 1 and 3, one can conclude that the dead zone manifest itself as a near cathode region with a pure real and positive resistance which is independent from the frequency up to the plasma range, and the end of the dead zone coincides with the maximum value of velocity overshoot. The remaining part of the n-region, where SNDC takes place, can be considered as the active region of the diode. By increasing the frequency, the active region with negative values of $Re[\nabla Z(f)]$ appears at first close to the anode and then widens and shifts towards the cathode. There, at sufficiently high frequencies several spatial regions with $Re[\nabla Z(f)] < 0$ can appear. In general, the maximum number of active regions which shows up in the spatial dependence of $Re[\nabla Z(f)]$ is equal to the number of generation bands in the frequency dependence of $Re[Z(f)]$. It due to the fact that the curves in Fig. 3 correspond to the growing space-waves of the local electric field starting at the beginning of the active zone and vanishing at the anode contact.

Figure 4 reports the effect of a reduction of the n region length on $Re[\nabla Z(f)]$ calculated at $f_3 = 290\ GHz$. Curve 1 corresponds to $l_n = 1.0\ \mu m$ and curve 2 to $l_n = 0.9\ \mu m$ when the anode n^+-region is shifted to the left up to the first nearest point in which $Re[\nabla Z(f)]$ vanishes. We observe that, in doing so, the second generation band disappears, the new profile practically coincides with curve 1 in the common region, and only one active zones followed by a zone with positive values of $Re[\nabla Z(f)]$ remains. Moreover, $Re[Z(f)]$ of the whole diode becomes positive at $f_3 = 290\ GHz$ (see curve 2 in Fig. 2). To make $Re[Z(f)]$ at this frequency negative again, it is necessary to shift the n^+-anode contact to the second point where $Re[\nabla Z(f)]$ crosses the zero axis. This case is illustrated by curves 3 in Fig. 4 (analogously as in Figs. 1 and 2) which is calculated for $l_n = 0.72\ \mu m$. In this way one removes the near-anode region with $Re[\nabla Z(f)] > 0$ and, as a consequence, the diode can again generate at frequency $f_3 = 290\ GHz$ since its $Re[Z(f_3)]$ becomes again negative (see Fig. 4, curve 3). The generation band of the shorted diode is so extended to the higher frequency range which fully covers the second generation band of the initial diode.

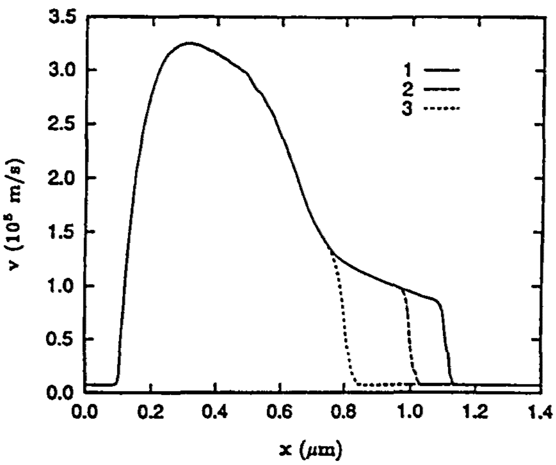

Fig. 1 - Spatial profiles of the drift velocity calculated for n^+nn^+ InP diodes with different n-region length l_n : $1 - 1.0\ \mu m$, $2 - 0.9\ \mu m$, $3 - 0.72\ \mu m$ (curves 1 to 3, respectively).

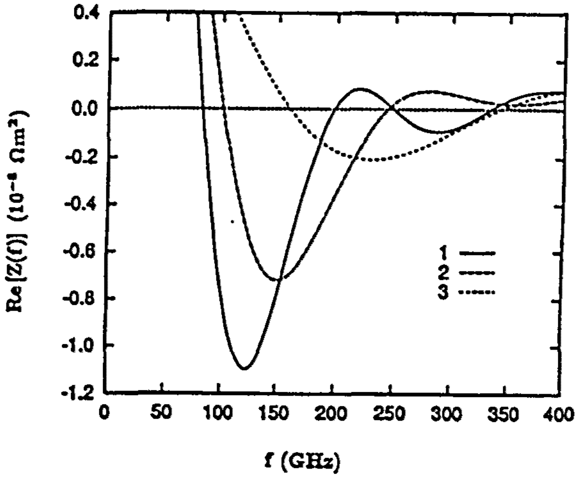

Fig. 2 - Frequency dependence of the real part of the small-signal impedance. The notation is the same of Fig. 1.

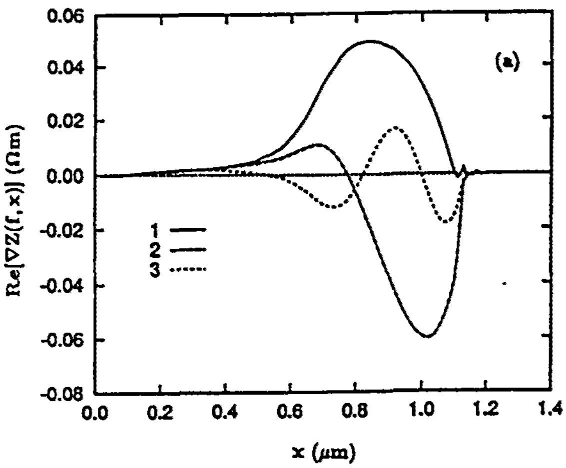

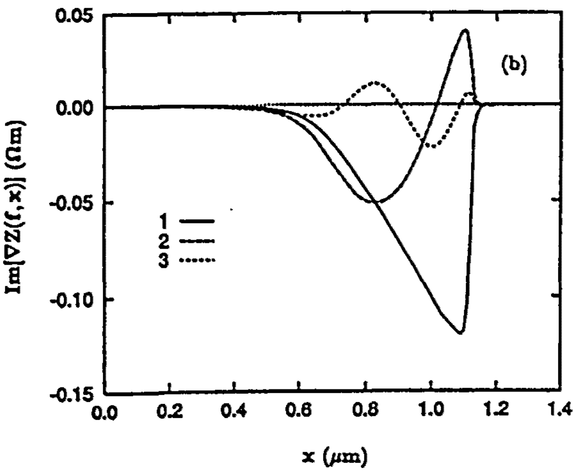

Fig. 3 - Spatial profiles of (a) the real and (b) imaginary part of the impedance field calculated with the HD approach for the n^+nn^+ InP diode of Fig. 1 with $l_n = 1.0\ \mu m$ at three different values of the frequency: $1 - 55\ GHz$, $2 - 125\ GHz$, $3 - 290\ GHz$. $l_n = 1.0\ \mu m$. $U_d = 8\ V$.

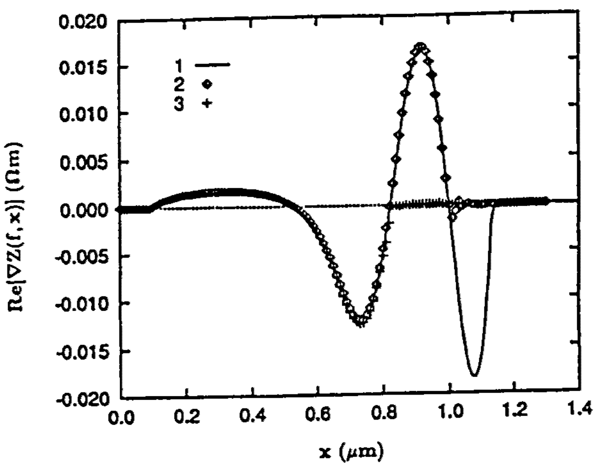

Fig. 4 - Spatial profiles of the real part of the impedance field calculated at the frequency $f = 290\ GHz$. The notation is the same of Fig. 1.

IV. CONCLUSIONS

The spatial dependence of the impedance field we have obtained in the whole frequency range of interest constructs a map which reflects the main physical processes occurring in the different regions of the device and can be used for several purposes such as: to give a comprehensive analysis of the device performance, to provide a proper choice of the device design, etc. Under current operation mode, the diode can be considered as a sequence of seriesly connected zones which give additive contributions to the amplification (and generation) spectrum. Each contribution can be described by a local impedance-field. Moreover, since the carrier flux starts at the source and ends at the drain, the local characteristics depend on the pre-history of carrier motion from the source only and contain no information about a further motion of carriers towards the drain.

References

[1] A. Rydberg, Electron Dev. Lett., **11**, 439 (1990).

[2] R. Kamoua, H. Eisele, G.I. Haddad, Solid-State Electron., **36**, 1547 (1993).

[3] H. Tian, et al., J. Appl. Phys., **72**, 5695 (1992).

[4] V. Gruzhinskis, et al., Appl. Phys. Lett., **61**, 1456 (1992).

[5] V. Mitin, V. Gruzhinskis, E. Starikov, P. Shiktorov, J. Appl. Phys., **75**, 935 (1994).

[6] V. Gruzhinskis, et al., SISDEP **5**, 333 (1993).

[7] V. Gruzhinskis, E. Starikov, P. Shiktorov, Solid-State Electron., **36**, 1055 (1993).

[8] V. Gruzhinskis, E. Starikov, P. Shiktorov, Solid-State Electron., **36**, 1067 (1993).

[9] V. Gruzhinskis, et al., Semicond. Sci. Technol., **8**, 1283 (1993).

[10] V. Gruzhinskis, et al., Noise in physical systems and 1/f fluctuations, P. H. Handel and A. L. Chung eds., AIP Press, New York, 1993, p. 312.